

2 **Development of anti-TNFR antibody-conjugated** 3 **nanoparticles**

4 **Ahmed Aido**^{1,2,*}, **Harald Wajant**², **Matej Buzgo**¹ and **Aiva Simaite**¹

5 Published: date

6 Academic Editor: name

7 ¹ InoCure s.r.o, R&d Lab, Prumyslová 1960, 250 88 Celákovice, Czech Republic; aiva@inocure.cz8 ² Division of Molecular Internal Medicine, Department of Internal Medicine II, University
9 Hospital Würzburg, Auverhaus, Grombühlstrasse 12, 97080 Würzburg, Germany;
10 harald.wajant@mail.uni-wuerzburg.de11 * Correspondence: ahmed@inocure.cz; Tel.: +49-174-913-6442

12 **Abstract:** Immunotherapy is considered as a new pillar of cancer treatment. However, the
13 application of some promising immunotherapeutic antibodies, such as antibodies against certain
14 immune-stimulatory receptors of the TNF receptor superfamily (TNFRs) including CD40, 41BB,
15 CD27 and anti-fibroblast growth factor-inducible 14 (anti-Fn14) are limited due to their low
16 bioactivity. It has been previously shown that the bioactivity of such anti-TNFR antibodies could be
17 improved by crosslinking or attachment to the plasma membrane by interaction with Fc γ receptors
18 (Fc γ R). Both result in proximity of multiple antibody-bound TNFR molecules what allows activation
19 of proinflammatory signaling pathways. In this work, we have grafted antibodies on gold
20 nanoparticles to simulate the “activating” effect of Fc γ R-bound and thus plasma membrane-
21 presented anti-TNFR antibodies. We have developed and optimized the method for the preparation
22 of gold nanoparticles, their functionalization with poly-ethylene glycol (PEG) linkers, and grafting of
23 antibodies on the surface. We showed here that antibodies, including the anti-Fn14 antibody PDL192,
24 can be successfully attached to nanoparticles without affecting antigen binding. We hypothesize that
25 conjugation of monoclonal anti-TNFR antibodies to the inorganic nanoparticles is a promising
26 technique to boost the efficacy of these immunotherapeutic antibodies.

27 **Keywords:** Nanoparticles; Surface modification; Drug-delivery, agonistic anti TNFRSF receptor
28 (TNFR) antibody
29

30 **1. Introduction**

31 Cancer immunotherapy is a very attractive field with high promise to provide cures for difficult
32 cancers. Immunotherapy relies on the stimulation or silencing of signaling pathways of relevance for
33 tumour development. Some of the promising immunotherapeutics target tumor necrosis factor
34 receptor superfamily (TNFRSF) receptors (TNFRs) which are naturally involved in the regulation or
35 even the inhibition of tumor growth [1]. The interactions between the ligands of the TNF superfamily
36 (TNFSF) and their TNFRs regulate innate and adaptive immune responses including natural killer
37 cell activation, T cell co-stimulation, and control of B cell homeostasis [1]. However, there are many
38 obstacles in the production of recombinant soluble TNFSF ligands and they show poor
39 pharmacokinetics (low serum half-life of only around 10–30 min) [2]–[4]. Thus, agonistic antibodies
40 targeting TNFRs such as CD40-, 41BB, CD27 and Fn14 are considered as alternative TNFR agoists to
41 soluble TNFSF ligand molecules. Unfortunately, anti-TNFR antibodies targeting a subgroup of
42 TNFRs including CD40, 41BB, CD27 and Fn14 typically lack agonistic activity as free molecules.
43 Instead, Fc γ R binding is required for these antibodies in order stimulate receptor signaling [5].

44 Medler *et al.* have shown that “activating” Fc γ R-dependent cell surface anchoring of IgG
45 antibodies can be replaced by anchoring domains genetically fused to antibodies that recognized cell
46 surface exposed structures distinct from Fc γ Rs [4]. We hypothesized that the activating effects of
47 plasma membrane associated presentation of antibodies can be simulated by grafting of antibodies
48 to a solid support. In this work, we have developed and optimized a method for attaching antibodies
49 to gold nanoparticles with the expectation to increase their activity.

50 Gold nanoparticles (AuNPs) are widely used in different biomedical applications and are used
51 as a platform for nanobiological conjugates, such as oligonucleotides [6], antibodies [7] and proteins
52 [8]. In addition, the physicochemical and optoelectronic properties of the spherical AuNPs such as
53 surface plasmon resonance, conductivity, large surface-to-volume ratio, excellent biocompatibility,
54 and low toxicity extend the possibilities to exploit them as new generation of drug delivery systems
55 [9]. All these properties combined, make gold nanoparticles a promising tool to deliver the
56 therapeutic agents to the targeted cells. In this work, we hypothesize that gold nanoparticles can be
57 exploited as a platform to immobilize antibodies against TNFRs, to enhance their agonistic activity.
58 More specifically, we used a known gold nanoparticle synthesis protocol and optimized for grafting
59 of antibodies, including the anti-Fn14 antibody PDL192, under preservation of their antigen binding
60 abilities.

61 2. Experiments

62 2.1. Materials

63 Gold (III) chloride acid trihydrate was obtained from VWR International. mPEG-SH / mPEG-
64 Thiol (5kDa) and SH-PEG-COOH / Thiol-PEG-Acetic Acid (5 kDa) were obtained from Biochempeg.
65 38.8 mM, trisodium citrate, 1-ethyl-3-(3-dimethylaminopropyl)carbodiimide hydrochloride (EDC)
66 were obtained from Thermo Scientific™, N-Hydroxysuccinimide(1-hydroxy-2,5 pyrrolidinedione)
67 (NHS) was obtained from Sigma-Aldrich, β -(N-Morpholino)ethansulfonsaure (MES), water free
68 $\geq 99\%$ and was obtained from VWR chemicals. 50 mM TRIS with 0.33 mg/ml mPEG-SH was used as
69 a blocking buffer.

70 The following antibodies were used: Humira (anti TNF alpha), Cosentyx® (IL-17A monoclonal
71 antibody) and anti-Fn14 PDL192. GpL-TNC-TNF has been described elsewhere (Lang et al., 2016) [10]
72 Fn14ed-GpL was generated by cloning the Gaussia princeps luciferase w/o leader to the C-terminus
73 of the extracellular domain of Fn14.

74 2.2. Methods

75 2.2.1. AuNPs synthesis:

76 The protocol for AuNP synthesis was adapted from [11], [12] with slight modifications. 100 ml
77 of 0.4 mM chloroauric acid solution was boiled in a clean 300-ml glass flask with stir bar. A reflux
78 column was attached on top of the flask to prevent the decrease of the solution’s volume. The entire
79 apparatus was placed on a hot plate and boiled while stirring. One ml of 38.8 mM trisodium citrate
80 solution was added to the solution to produce 60 nm spherical monodisperse gold nanoparticles.
81 Other sizes were created based on the amount of added trisodium citrate and/or the concentration of
82 auric salt within a range between 15 and 100 nm. Upon addition of the trisodium citrate, the colour
83 of the solution change to blue in about 30 s and then to red in another 150 s. The colour change during
84 synthesis is attributed to the increase in size of gold nanoparticles as the citrate ions reduce the gold
85 ions [13]. The boiling was continued for another 10 min and then cooled to room temperature.

86 2.2.2. AuNPs functionalization:

87 To modify the surface of the produced gold nanoparticles with functional carboxyl groups, a
88 volume of HS-PEG-COOH solution with a selected concentration was added to the whole amount of
89 the produced colloidal of AuNPs to get 100 ug/ml of HS-PEG-COOH in the solution and was left to
90 be mixed for one hour. The whole amount of carboxyl-modified AuNPs was centrifuged in a big
91 centrifuging device (10000 RPM for 10 min) then the pellet was collected in an Eppendorf tube and

92 washed twice with mPEG (0.33 mg/ml) (in order to fill the unmodified places on the surface of
93 HOOC-PEG-AuNPs and to compensate the washed stabilizer trisodium citrate).

94 2.2.3. AuNPs grafting:

95 The carboxyl-modified AuNPs were conjugated with the protein of interest according to the
96 EDC-NHS covalent binding procedure adapted from [14]–[18]. Briefly, an amount of purified C-
97 AuNPs were resuspended in a volume of the activation/coupling buffer (50 mM MES, pH 6.0) and
98 washed with it for 3 times. Then, 24 μ L of EDC (200 mM) and 240 μ L of NHS (200 mM) were added
99 to 1 ml of the previous solution of AuNPs, and incubated for 30 min in RT. After washing the particles
100 from the EDC and NHS reagents for 3 times with the activation/coupling buffer, 500 μ l of the
101 activated C-AuNPs were incubated with 500 μ l of a selected concentration of the protein of interest
102 (anti-TNF, anti-Fn14, anti-IL17A). The antibody-grafted AuNPs were washed from the excess of the
103 unconjugated protein for 3 times with the blocking buffer (Tris 50 mM in mPEG-SH (0.33 mg/ml)) to
104 block the free activated carboxyl sites on the surface of gold nanoparticles. Finally, the antibody-
105 grafted AuNPs were resuspended in a volume of the blocking buffer to be ready for later on
106 application.

107 2.2.4. Characterization

108 UV-Vis: AuNPs samples were collected at each stage immediately after synthesis and their
109 optical properties were evaluated by UV-vis spectrophotometry (SpectraMax.). The absorption
110 spectra were acquired in the range of 450–650 nm with a step of 5/10 nm.

111 DLS: The size of the obtained AuNPs (unPEGylated, PEGylated and grafted particles) were
112 analyzed, using the Nanophox 123 Dynamic Light Scattering (DLS) with photon cross-correlation
113 spectroscopy from Sympatec. The particles were purified by centrifugation at 22,000 g for 10 min,
114 diluted 100 times in distilled water, then analyzed. All DLS experiments were carried out at a
115 temperature of 25°C.

116 Zetasizer : The effective surface charges on the gold nanoparticles were measured using zeta-
117 potential (Malvern Instruments Zetasizer). Reported zeta potential measurements were collected on
118 aqueous solution in which AuNPs were diluted 10-100 times depending on their concentration .

119 3. Results

120 3.1. Optimization of gold nanoparticles synthesis protocol

121 3.1.1. Controlling the size and concentration of gold nanoparticles

122 The size of AuNPs can be adjusted by controlling the concentration of the auric salt (HAuCl_4
123 $\cdot 3\text{H}_2\text{O}$) [12]. To optimize the procedure for the preparation of AuNPs needed for our work, that is in
124 order to obtain AuNPs with the size below 200 nm, we have set trisodium citrate concentration to
125 38.8 mM and varied the concentration of gold chloride and boiling duration. UV-vis absorption was
126 used to characterize the particles size (the wavelength of the maximum absorbance of the plasmon
127 band of the spherical particles AuNPs are in dependence of the particles size [19]. As shown in **Figure**
128 **1a**, increasing the concentration of the gold chloride leads to the λ_{max} shift from 520 nm to 550
129 nm, indicating the increase of particle size from 15 nm to 80 nm. On the other hand, different results
130 were noted for the influence of the boiling duration. In this case the λ_{max} absorbance of the colloidal
131 solution was measured after 5, 20 and 40 min of boiling. As shown in **Figure 1b**, the optical density
132 increased with fixed λ_{max} absorbance indicating that the total amount of the produced gold
133 nanoparticles increased with the continuing boiling [13].

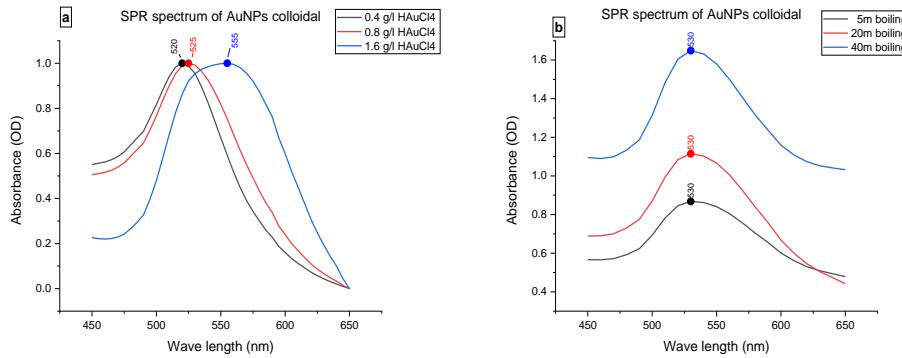


Figure 1: λ_{max} absorbance of the (SPR) of AuNPs colloidal. Comparison between spectrum of the absorbance of AuNPs colloidal resulted from a) different concentration of HAuCl₄ · 3H₂O. or b) different boiling duration.

134 3.1.2. Functionalization of the gold nanoparticles

135 Trisodium citrate plays a role as reducing agent and a stabilizer of the produced gold nanoparticles
 136 [20]. The abundance of the negative charges of the citrate structure surrounding the surface of AuNPs
 137 is known to prevent their aggregation. However, the stabilization effect of citrate is not significant
 138 enough for storing the particles long term and can be lost after the purification. To increase the long
 139 term stability of the AuNPs and to introduce chemical groups for the subsequent functionalization,
 140 particles were functionalized with a layer of SH- and carboxyl- (5 kDa HOOC-PEG-SH) or methoxy-
 141 (5 kDa H₃C-O-PEG-SH) containing polymers. Grafted particles were purified by washing with distilled
 142 water to discard the excess of trisodium citrate and free polymer molecules. As indicated in Figure 2,

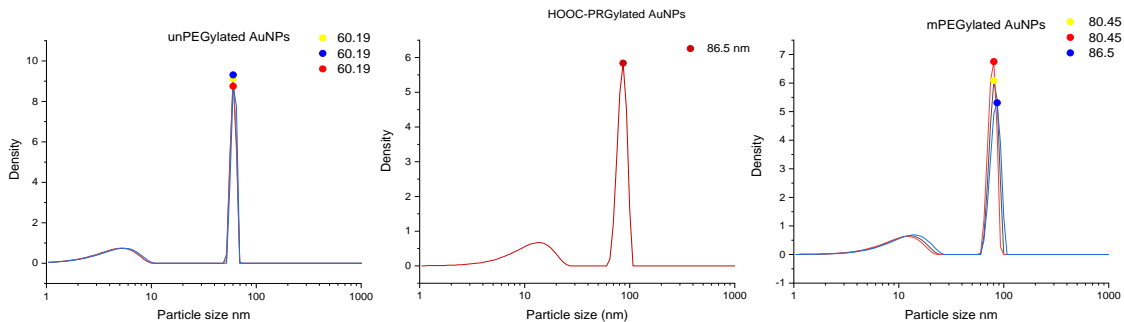


Figure 2: Diameter distribution graphs from DLS show the increase of particles size after PEGylation with carboxyl-PEG-SH and mPEG-SH

143 the increase of particles size after the PEGylation grafted with two types of polymers is similar, most
 144 likely due to the identical molecular weight. To confirm the PEGylation, zeta potential measurements
 145 were performed. As shown in Table 1, the PEGylation leads to a change in ζ potential values. In
 146 comparison to the citrate stabilization, the dominant charge of the particles after PEGylation is even
 147 more negative after PEGylation with the carboxyl- terminated polymer (-20 mV), and less negative
 148 when methoxy-PEG was used (-7 mV).

149 **Table 1:** Comparison of ζ potential values and particles size between the un-PEGylated and PEGylated gold
 150 nanoparticles.

Sample structure	Particles Size	ζ potential
Trisodium citrate - AuNPs	60.19 nm	-14 mv
mPEG-AuNPs	80.45 nm	-7 mv
HOOC-PEG-AuNPs	86.5 nm	-20 mv

151 3.2. Characterization the conjugation of C-AuNPs with different therapeutic antibodies
 152 Carboxyl-modified gold nanoparticles C-AuNPs (ca. 60 nm, 25 mg/ml) were conjugated with the
 153 following proteins: anti-Fn14 antibody PDL192, anti-TNF or anti-IL17A. The conjugation process was
 154 performed by following the EDC/NHS covalent coupling procedure (described in the methods). To
 155 confirm not only the conjugation of C-AuNPs with the antibodies but also their post-conjugation
 156 functionality, binding studies using the antigens TNF and Fn14 fused to the Gaussia princeps

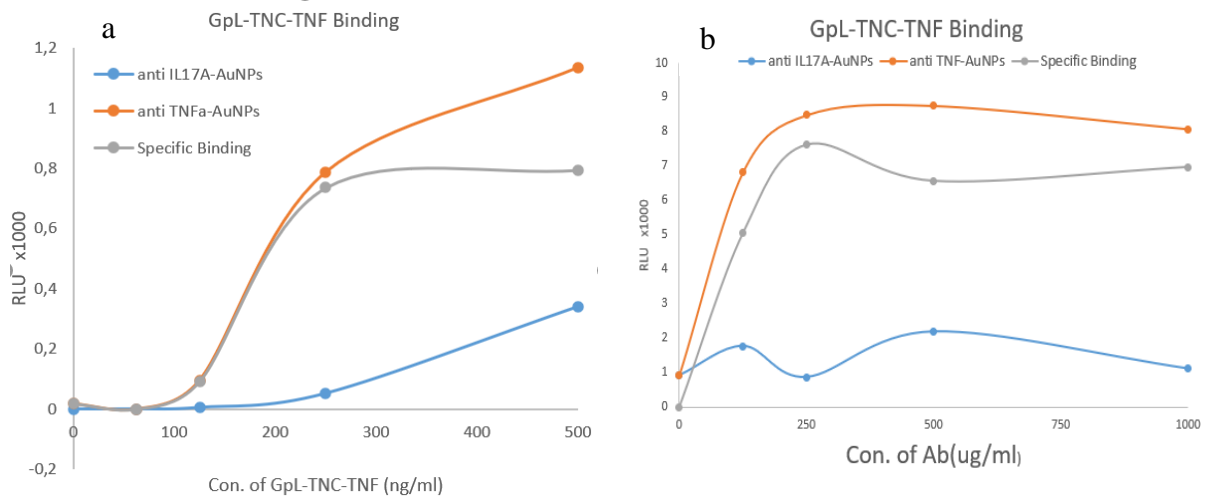


Figure 3: Binding of GpL-TNC-TNF fusion protein to either anti-TNF-AuNPs or anti-IL17A-AuNPs: Carboxyl-modified gold nanoparticles C-AuNPs (ca. 60 nm, 25 mg/ml) were conjugated with either fixed concentration of anti-TNF or anti-IL17A. Then binding studies have been carried out with serial dilutions of GpL-TNC-TNF (a). Alternatively, different concentrations of the two antibodies were used for gold nanoparticle conjugation and GpL-TNF-TNC binding with a fixed concentration was analyzed (b). The curve of the specific binding was obtained by subtraction of the binding to anti-IL17A from the values of the binding to anti-TNF.

157 Luciferase (GpL-TNF-TNC, Fn14ed-GpL) [10]. The GpL domain allows the quantification of the
 158 binding to the corresponding gold nanoparticle associated antibodies by measurement of the
 159 luminescence upon removal of the free GpL fusion protein molecules. The binding curves between
 160 GpL-TNF-TNC and anti-TNF-AuNPs (total binding) or anti-IL17A-AuNPs (unspecific binding) are
 161 shown in **Figure 3a**. A serial dilution of the GpL-linked antigen (from 0 ng/ml to 500 ng/ml) were
 162 mixed with the fixed concentration (25 mg/ml) of the AuNPs conjugated with antibody (1mg/ml conc
 163 in linking solution). As show in the **Figure 3a**, in all cases, the luminescence increased with the
 164 increasing antigen concentration. However, notably higher binding was observed with anti-TNF than
 165 with anti IL17A AuNPs. This indicates high specific binding of GpL-TNC-TNF to gold nanoparticle
 166 immobilized anti-TNF. Thus the conjugation of the antibody did not notably affected the interaction
 167 between the conjugated Ab and its antigen.

168 In order to evaluate the maximum amount of the antibody that can be conjugated to the
 169 nanoparticles, increasing concentrations of anti-TNF or anti-IL17A were used for conjugation. The
 170 binding of a GpL-TNF-TNC solution with constant concentration was then determined as shown in
 171 **Figure 3b**. With a concentration of 250 ug/ml of anti-TNF in the coupling reaction the maximum
 172 amount of antibody could be immobilized on the particles. Increasing the antibody concentration did
 173 not lead to an further increase in antigen binding. Similar binding studies with anti-Fn14 PDL192-
 174 AuNPs and their GpL-fused antigen (Fn14ed-GpL) were performed. As shown in **Figure 4**, maximum
 175 conjugation capacity was again reached at the antibody concentration of 250 ug/ml – similar to the
 176 results shown in **Figure 3b**.

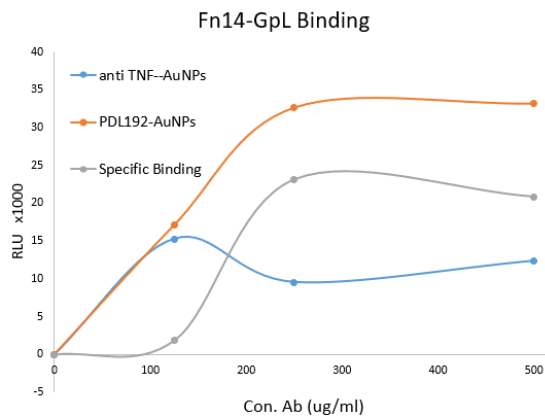


Figure 4: Binding of Fn14ed-GpL fusion protein to either antiTNF-AuNPs or PDL192 -AuNPs: Carboxyl-modified gold nanoparticles C-AuNPs (ca. 60 nm, 25 mg/ml) were conjugated with different concentration of the both antibodies and then the signals of the emitted light resulted from the binding with fixed concentration of Fn14ed-GpL were measured and plotted. The curve of the specific binding was obtained by subtraction of the binding to anti-TNF from the values of the binding to PDL192.

177 4. Discussion

178 Since the early work of Turkevich and Frens, method to produced gold nanoparticles in the
 179 scale, from 9 to 120 nm and with defined size distribution, have been optimized for various
 180 applications [13], [21]. Gold NPs can be coated with a ligand shell, which provides colloidal stability,
 181 or conjugated with (biological) molecules via thiols [22, Rivera-Gil *et al*]. However attaching Abs
 182 directly to the surface of NPs has drawbacks, that is, the process may affect their activity by blocking
 183 the active side. To overcome this problem, a method depending on directional covalent binding to a
 184 functional polymer on the surface of NPs has been investigated in the literature [23]. One effective
 185 method is the use of 1-ethyl-3-(3-dimethylaminopropyl) carbodiimide (EDC) chemistry [24].

186 Antibodies bear amine groups on some of their amino acid side chains including residues in the
 187 the antigen binding site. To detect the probability of the binding to antigen binding-irrelevant sites
 188 of the antibody, we functionalized AuNPs with carboxyl-containing polymer and then conjugated
 189 them with the therapeutic Abs using EDC/NHS chemistry, and carried out binding studies. The
 190 performed binding studies revealed that, even though some antibodies might have coupled through
 191 their antigen binding sites, other coupled through antigen binding irrelevant amino acids and remain
 192 active.

193 Recent studies found that specific antibodies to the TNF receptor Fn14, can mimic some effects
 194 of the soluble TWEAK, Fn14 specific TNF ligand, by triggering the related signaling pathways.
 195 However, the soluble anti-Fn14 antibody failed to activate all of the needed signaling pathways of
 196 the soluble TWEAK. This drawback of the soluble anti-Fn14 can be overcome by the oligomerization
 197 using protein G or by the anchoring to Fcγ receptors of the effector cells, which provides the antibody
 198 with agonistic activity [4], [25]. In the future work, we will exploit the gold nanoparticles as a
 199 platform to immobilize the therapeutic antibody (PDL192) as a model. We hypothesize that the
 200 AuNPs-conjugated anti Fn14 monoclonal IgG1 antibody will possess the agonistic activity which
 201 resembles the Fcγ receptors anchoring-dependent efficiency. Such anchored antibodies should then
 202 be able to trigger the associated proinflammatory signaling pathways. If successful, this approach
 203 will enable promising applications of nanocomposites with antitumor antibodies. Furthermore we
 204 will work on the nanoencapsulation of these nanoparticles to target tumor tissues specifically and
 205 prevent the systemic side effects associated with such antibodies.

206 5. Conclusions

207 Gold nanoparticles of diameter ca. 60 nm have been synthesized by sodium citrate reduction

- 247 substrate-functionalized gold nanoparticles,” *Chem. Commun. (Camb)*, no. 27, pp. 2905–2907, Jul. 2006.
- 248 [9] Y.-C. Yeh, B. Creran, and V. M. Rotello, “Gold nanoparticles: preparation, properties, and applications
- 249 in bionanotechnology,” *Nanoscale*, vol. 4, no. 6, pp. 1871–1880, Mar. 2012.
- 250 [10] I. Lang *et al.*, “Binding Studies of TNF Receptor Superfamily (TNFRSF) Receptors on Intact Cells *,”
- 251 vol. 291, no. 10, pp. 5022–5037, 2016.
- 252 [11] J. Kimling, M. Maier, B. Okenve, V. Kotaidis, H. Ballot, and A. Plech, “Turkevich method for gold
- 253 nanoparticle synthesis revisited,” *J. Phys. Chem. B*, vol. 110, no. 32, pp. 15700–15707, 2006.
- 254 [12] G. FRENS, “Controlled Nucleation for the Regulation of the Particle Size in Monodisperse Gold
- 255 Suspensions | Kopernio.” [Online]. Available:
- 256 [https://kopernio.com/viewer?doi=10.1038/physci241020a0&token=WzExNDE5NzUsIjEwLjEwMzgvG](https://kopernio.com/viewer?doi=10.1038/physci241020a0&token=WzExNDE5NzUsIjEwLjEwMzgvGh5c2NpMjQxMDIwYTAiXQ.es09awC7jdG9BahFkjNV3cCqjpQ)
- 257 [h5c2NpMjQxMDIwYTAiXQ.es09awC7jdG9BahFkjNV3cCqjpQ](https://kopernio.com/viewer?doi=10.1038/physci241020a0&token=WzExNDE5NzUsIjEwLjEwMzgvGh5c2NpMjQxMDIwYTAiXQ.es09awC7jdG9BahFkjNV3cCqjpQ). [Accessed: 16-Dec-2019].
- 258 [13] W. Haiss, N. T. K. Thanh, J. Aveyard, and D. G. Fernig, “Determination of size and concentration of gold
- 259 nanoparticles from UV-Vis spectra,” *Anal. Chem.*, vol. 79, no. 11, pp. 4215–4221, Jun. 2007.
- 260 [14] A. J. Lomant and G. Fairbanks, “Chemical probes of extended biological structures: synthesis and
- 261 properties of the cleavable protein cross-linking reagent [35S]dithiobis(succinimidyl propionate),” *J.*
- 262 *Mol. Biol.*, vol. 104, no. 1, pp. 243–261, Jun. 1976.
- 263 [15] Z. Grabarek and J. Gergely, “Zero-length crosslinking procedure with the use of active esters,” *Anal.*
- 264 *Biochem.*, vol. 185, no. 1, pp. 131–135, Feb. 1990.
- 265 [16] N. Nakajima and Y. Ikada, “Mechanism of Amide Formation by Carbodiimide for Bioconjugation in
- 266 Aqueous Media,” *Bioconjug. Chem.*, vol. 6, no. 1, pp. 123–130, 1995.
- 267 [17] J. V. Staros, “Membrane-Impermeant Cross-Linking Reagents: Probes of the Structure and Dynamics of
- 268 Membrane Proteins,” *Acc. Chem. Res.*, vol. 21, no. 12, pp. 435–441, 1988.
- 269 [18] J. V. Staros, R. W. Wright, and D. M. Swingle, “Enhancement by N-hydroxysulfosuccinimide of water-
- 270 soluble carbodiimide-mediated coupling reactions,” *Anal. Biochem.*, vol. 156, no. 1, pp. 220–222, 1986.
- 271 [19] L. Đorđević, F. Arcudi, and M. Prato, “Preparation, functionalization and characterization of engineered
- 272 carbon nanodots,” *Nat. Protoc.*, vol. 14, no. 10, pp. 2931–2953, Oct. 2019.
- 273 [20] J. P. Oliveira *et al.*, “A helpful method for controlled synthesis of monodisperse gold nanoparticles
- 274 through response surface modeling,” *Arab. J. Chem.*, 2020.
- 275 [21] L. M. Liz-marz, “Nanometals ;,” no. February, pp. 26–31, 2004.
- 276 [22] J. Montenegro *et al.*, “Controlled antibody / (bio-) conjugation of inorganic nanoparticles for targeted
- 277 delivery ☆,” *Adv. Drug Deliv. Rev.*, 2013.
- 278 [23] G. Hermanson, *Bioconjugate Techniques*, 2nd Editio. .
- 279 [24] D. Bartczak and A. G. Kanaras, “Preparation of peptide-functionalized gold nanoparticles using one pot
- 280 EDC/Sulfo-NHS coupling,” *Langmuir*, vol. 27, no. 16, pp. 10119–10123, 2011.
- 281 [25] S. Salzmann *et al.*, “Fibroblast growth factor inducible (Fn14)-specific antibodies concomitantly display
- 282 signaling pathway-specific agonistic and antagonistic activity,” *J. Biol. Chem.*, vol. 288, no. 19, pp. 13455–
- 283 13466, 2013.

284 © 2020 by the authors; licensee MDPI, Basel, Switzerland. This article is an open access article distributed under

285 the terms and conditions of the Creative Commons by Attribution (CC-BY) license



[\(http://creativecommons.org/licenses/by/4.0/\)](http://creativecommons.org/licenses/by/4.0/).